

# Simulating Cooperative Systems Applications: a New Complete Architecture

Dominique Gruyer  
IM-LIVIC, IFSTTAR  
Versailles, France

Sébastien Demmel  
CARRS-Q, Queensland University of Technology  
Kelvin Grove (QLD), Australia

Brigitte d'Andréa-Novel  
CAOR – Centre de Robotique, MINES ParisTech  
Paris, France

Grégoire S. Larue and Andry Rakotonirainy  
CARRS-Q, Queensland University of Technology  
Kelvin Grove (QLD), Australia

**Abstract**—For a decade, embedded driving assistance systems were mainly dedicated to the management of short time events (lane departure, collision avoidance, collision mitigation). Recently a great number of projects have been focused on cooperative embedded devices in order to extend environment perception. Handling an extended perception range is important in order to provide enough information for both path planning and co-pilot algorithms which need to anticipate events. To carry out such applications, simulation has been widely used. Simulation is efficient to estimate the benefits of Cooperative Systems (CS) based on Inter-Vehicular Communications (IVC). This paper presents a new and modular architecture built with the SiVIC simulator and the RTMaps™ multi-sensors prototyping platform. A set of improvements, implemented in SiVIC, are introduced in order to take into account IVC modelling and vehicles' control. These 2 aspects have been tuned with on-road measurements to improve the realism of the scenarios. The results obtained from a freeway emergency braking scenario are discussed.

**Keywords**—Cooperative Systems; IEEE 802.11p; Inter-vehicular Communications; simulation

## I. INTRODUCTION

Cooperative Systems (CS) are widely considered as the next major step in driving assistance systems (ADAS), aiming at increasing safety and comfort for drivers [1] Wireless Inter-Vehicular Communications (IVC) are used to share information so that drivers, or ADAS, can enhance their awareness of their surroundings. The state of the vehicle or the driver, detected objects and events pertaining to the driving environment (ranging from traffic and weather information to collision warning) are the type of information that can be exchanged within Vehicular Ad-hoc Networks (VANETs). A straightforward example of cooperative systems is Emergency Electronic Brake Light [2] (EEBL): a piece of information which is naturally available within a certain distance, i.e. a vehicle's break lights, is extended to a larger area of perception through IVC. Cooperative Collision Warning (CCW) can be achieved with EEBL by broadcasting a warning message whenever a vehicle is performing an emergency braking manoeuvre.

Development of CS requires additional resources in terms of extended perception which are both time-consuming and

expensive. Therefore, it becomes essential to have a simulation environment or platform that allows prototyping and evaluating extended, enriched and cooperative ADAS in the early stages of the system's design. This virtual simulation platform has to integrate models of road environments, virtual on-vehicle sensors (proprioceptive & exteroceptive), infrastructure-based sensors and IVC devices, which are all consistent with the laws of physics. Similarly, a physics-based model for vehicular dynamics coupled with actuators (steering wheel angle, torques on each wheel) is required. Within such a platform, it becomes possible to simulate accurately the performance of future cooperative ADAS.

This paper presents an architecture to simulate and evaluate CS applications, based on the functionalities of both the SiVIC and RTMaps™ interconnected platforms [3], [4]. Such coupling allows meeting the aforementioned requirements. Our CS simulation architecture brings several improvements to the SiVIC-RTMaps™ coupling, regarding the modelling of IVC and vehicle's control.

The existing transponder-like behaviour of IVC simulation in SiVIC [5] is extended to a more realistic modelling with data from actual on-tracks measurements with prototype 802.11p devices. IEEE 802.11p [6] is the leading IVC technology that has been pushed forward by the IEEE for short-to-medium range communications (up to one kilometre), for both Vehicle-to-Vehicle (V2V) and Vehicle-to-Infrastructure (V2I) communications. To evaluate cooperative ADAS, especially when safety-critical tasks are concerned, it is necessary to be able to simulate 802.11p actual behaviour. Indeed, cooperative ADAS specifications and actual performance will be strongly affected by how 802.11p behaves on the road. Unfortunately, its performance is likely to diverge from that studied in earlier theoretical simulations, upon which most models are based, as we have shown in [7]. A safety-focused cooperative ADAS could have less benefit than we could expect in a real setting where IVC performance are overestimated.

Empirical modelling is a good way to improve simulations' accuracy by taking into account all existing perturbation sources. Thus, we have extended our transponder-like simulation so that it can have sufficient performance to emulate 802.11p. The new model outputs range, frame loss

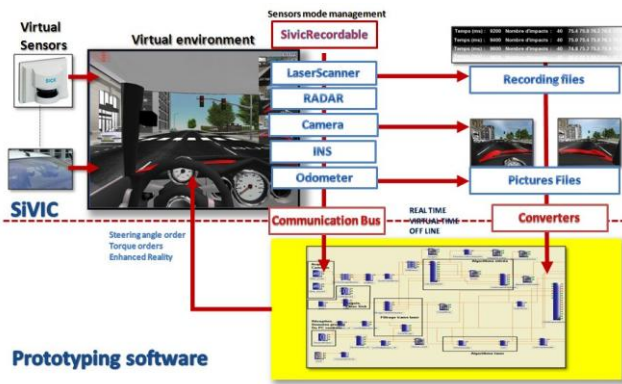


Fig. 1. General architecture of ADAS prototyping with SiVIC

and latencies, which are classified along the relative speed between vehicles and/or roadside units. Hardware

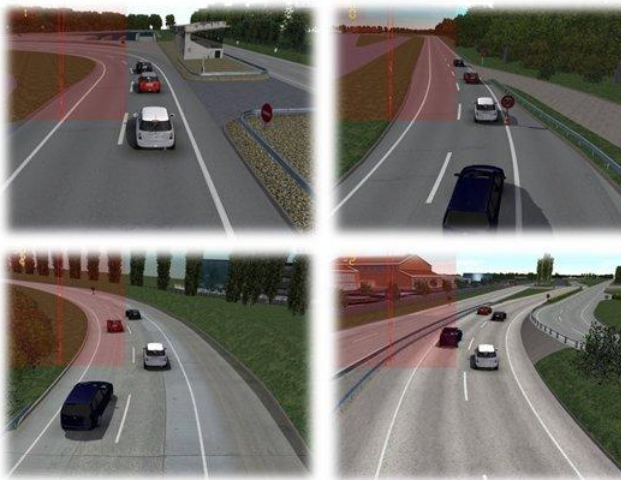


Fig. 2. Multiple captures from the Versailles-Satory's test tracks scenery; SiVIC's visual rendering is focused on generating accurate image dynamic, rather than merely acceptable realism to human eyes

inhomogeneities, ground reflections, multipath effects on vegetation and other objects, as well as the weather, are factors that influence the outputs. We have based our modelling on data collected on over 400 km of driving on Versailles-Satory's test tracks (near Paris, France) in late 2011 and early 2012.

Several improvements are also be made to the vehicle's controllers comparing to previous versions developed for the Full Range Speed Acc and Lane Keeping applications [8], in order to have a closer-to-life simulation of a human driver as well as introducing mechanisms related to CCW, such as emergency braking manoeuvres.

Our architecture can be used, for example, to evaluate the impact of introducing IVC devices into a driving situation leading to crashes, compared to using non-cooperative ADAS, or without any ADAS altogether. To demonstrate that our architecture can be used to produce meaningful results, we will show how an EEBL application can be simulated with it.

In order to validate it, we have found that our application reproduces results from previous larger scale simulations [9], [10].

The remainder of this paper is organised as follows: Section II presents the CS simulation architecture we have developed, including software mechanisms in SiVIC and RTMaps™, the 802.11p IVC modelisation and our control's equations. Section III focuses on an application of our architecture, presenting detailed results analysing the effects a CS-based ADAS has on crash number and severity. Finally, we give few words of conclusion and perspective on future works in Section IV.

## II. COOPERATIVE SYSTEMS SIMULATION ARCHITECTURE

### A. SiVIC-RTMaps™ interconnection

Our CS simulation architecture is based on the interconnection of the sensors simulation platform SiVIC and the prototyping platform RTMaps™. The interconnection between SiVIC and RTMaps™ allows replacing real measurements by simulated ones, creating a fully Software-In-Loop (SIL) development and prototyping approach.

#### 1) The SiVIC platform

SiVIC [3] is a platform designed to enhance the process of developing and evaluating ADAS. This platform enables the simulation of multi-frequency sensors embedded in static or dynamic devices, equipments and vehicles commonly used in ADAS scenarios.

The SiVIC platform is a very efficient tool to develop, prototype and evaluate high level ADAS (see Fig. 1), including CS applications. SiVIC can be easily interconnected with several external platforms such as RTMaps™ (see section II-A2) or Matlab™ (from Mathworks). This interconnection interface is efficient and useful to perform a great number of developments in a SIL approach. Once the application is evaluated in virtual condition and validated in simulation, it can be integrated and tested into a real embedded hardware architecture (on vehicle) further towards the end of the development cycle.

SiVIC uses a realistic graphical environment (Fig. 2), supported by physically accurate behaviours for vehicles and sensors. It can generate a flow of time-stamped and synchronised data that can be recorded and/or interacted with by prototyping and/or data treatment platforms such as RTMaps™ or Matlab™. Furthermore, SiVIC can generate multiple scenarios with events-driven mechanisms, so that the robustness and reliability of control and perception algorithms can be extensively tested on many parameters. This functionality is useful for scenarios featuring hazardous environments, complex situations, or missing or erroneous data (from sensors or actuators). Moreover, data analysis can always be performed with accurate ground truth references.

Proprioceptive and exteroceptive sensors are modelled in SiVIC so that, from the point of view of an algorithm, there is no difference between a fully SIL sensor and an on-vehicle sensor. Sensors available in SiVIC are:

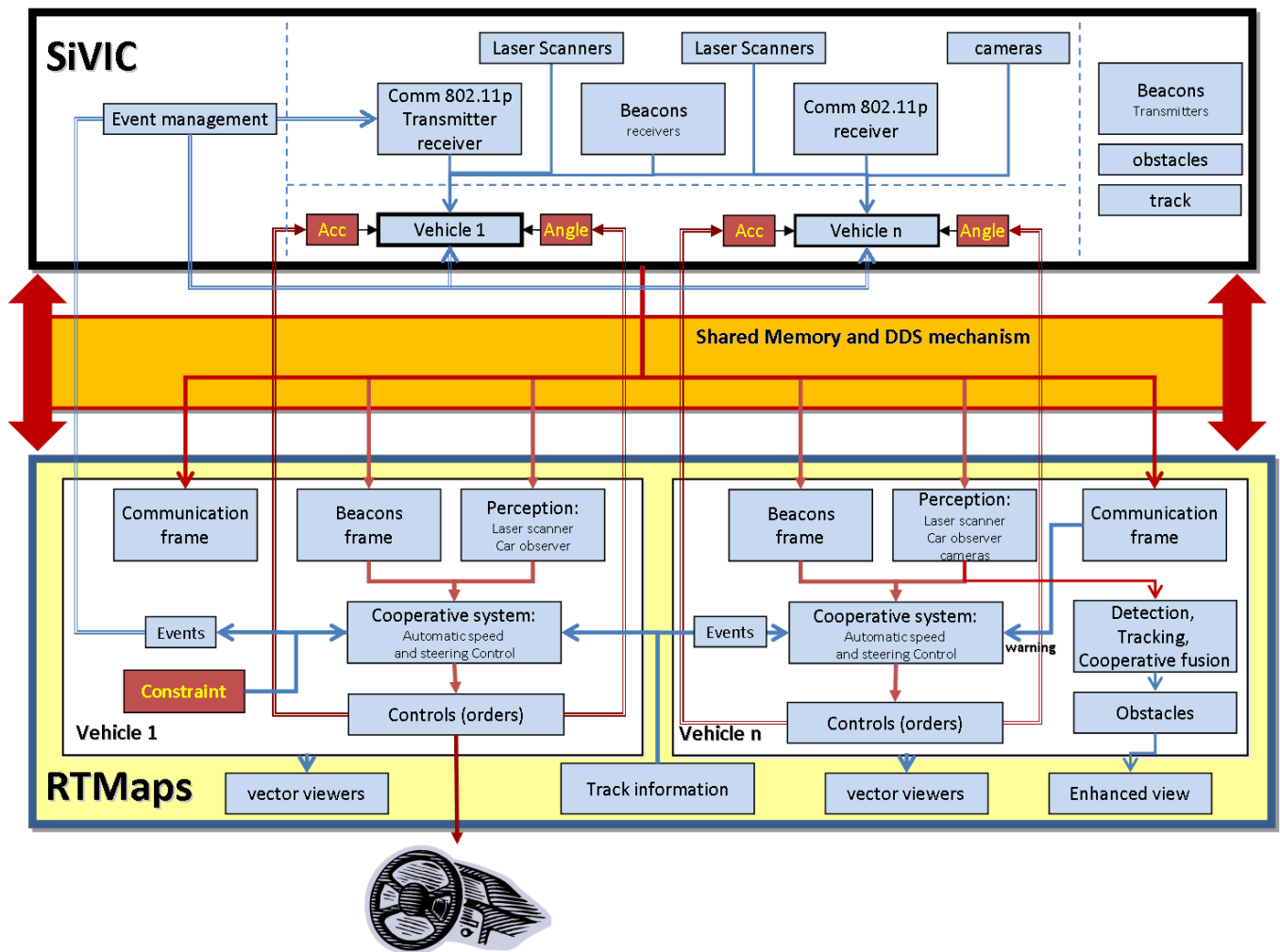


Fig. 3. CS simulation architecture's detailed functions in SiVIC-RTMaps™

- System variables (called observers) that provide output reference data on an object's position and behaviour
- Cameras (configurable either as software or hardware cameras), including Fisheye and omnidirectional cameras
- Inertial Navigation Systems (3 axes accelerometer + 3 axes gyrometer)
- Odometer
- Telemetric laserscanner (multi-layered, capable of using either ray-tracing or Z-Buffer methods)
- Radiofrequency transponders.

Additional sensors are being implemented in SiVIC at the moment and are close to deployment; most are related to the implementation of a realistic model of electromagnetic waves

propagation in the platform. They include a simulation of GPS, that goes up to the influence of satellite's ephemerides, and a radar. The Radiofrequency transponders have been already used for previous works on cooperative speed control by transponder-equipped infrastructure [5]. This work has been used and extended in the present paper to take advantage of a more realistic model of IVC behaviour, based on field measurements.

## 2) RTMaps™

RTMaps™ is marketed by Intempora<sup>1</sup>, based upon work undertaken at Mines ParisTech a decade ago [11]. Its primary goal is to record and process a large number of simultaneous data flows such as images, laserscanner scans, positioning data (from GPS, odometer or INS), etc. User-developed algorithms, for image processing or data fusion for example, can be deployed in the RTMaps™ framework in dedicated libraries called *packages*; packages themselves contain *components* to apply specific treatments to the data flow. Recorded data can be easily replayed, which is especially useful to precisely tune algorithms with multiple re-runs of a same on-tracks measurement.

<sup>1</sup> www.intempora.com

## B. Overall architecture

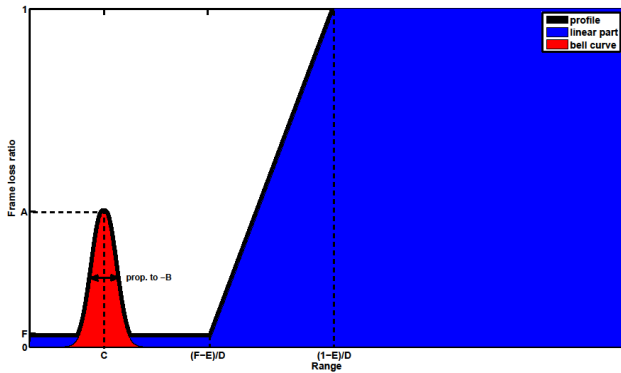


Fig. 4. Decomposition of a frame loss profile  $\tau$ , with its parameters

The developed CS simulation architecture can be applied to any kind of CS usage scenario. It is partially scenario-specific, both in SiVIC and RTMaps. Scenarios are built in SiVIC by using script files, that specify the location of objects and many other parameters. The actual CS application needs to be developed and implemented in RTMaps. While developing our architecture, in order to simplify our work, we focused at first on simulating strings of IVC-equipped vehicles, specifically for EEBL applications. However, developments such as vehicles' control mechanisms and the 802.11p simulation are not scenario-dependent and are an integral part of SiVIC.

Fig. 3 shows the data flow and relationships between the environment, sensors and algorithms as implemented in the SiVIC-RTMaps™ environment.  $veh_1$  is considered as the *leader*, and embeds a 802.11p modem used only for alert transmission, while the other vehicles ( $veh_n$ ) are *followers*, and embed 802.11p only used in reception. Apart from this distinction, one can see that each vehicle has identical features. Vehicles are controlled from/within RTMaps, with the combination of the *cooperative system* and *control* blocks, that use information shared via IVC and obtained from embedded sensors to control the vehicle's behaviour in SiVIC (from actuators on the wheels and steering wheel).  $veh_1$  can have additional control constraints, as required by the scenario.

## C. Pre-existing transponders simulation

The pre-existing transponders simulation is composed of two plug-ins, for transmission and reception; both are strictly one-way. Each plug-in can be attached to any object in the simulation, from vehicles to roadside objects. The simulation is driven from the receptor's point of view. Whenever prompted, a receptor will check all the transmitters loaded in the simulation to verify whether they are in range, as specified in the receptor's parameters. Each emitter within range will then transmit its data frame. It is possible to use several receptors on a single vehicle, and receive messages from different transmitters.

The transponders were programmed to use the same frame pattern as real equipments. In order to match this format, the transponder uses three types of data: bits, bytes and strings,

which are contained within a frame script. A frame script includes, for each line representing data, four fields: name, type, amount of data, and the actual data. Once these data are processed by the parser, a frame is produced. A receptor transponder decodes the frame pattern using the same algorithm as found in real devices.

## D. 802.11p enhanced simulation

As initially used in [5], the transponders' range was very limited (less than 20 metres), as they only had to provide speed regulation information to passing vehicles. By extending the transponders' range, it was possible to get a simple simulation of IVC. However, this simulation was not representative of what would happen on a real road. Indeed, on the road, many factors will compound to alter the range of IVC and introduce errors that lead to frame loss, depending on the nature of objects inside the environment, weather, vehicles' behaviour, etc. Additionally, the existing transponders simulation did not include latencies, which, depending on the type of IVC used and the range of communication, can become non-negligible considering SiVIC's simulation step (fixed at 5 milliseconds in the current work).

Using data collected on the Versailles-Satory's test tracks during autumn and winter 2011-12 [7], we developed a new, more accurate 802.11p-based IVC model that introduces realistic IVC defects. The model covers the following sources of defects: multi-path reflections from the ground, from objects and vegetation, from weather, and from hardware inhomogeneities. Although they are accounted for in the model, these sources of performance variations cannot be differentiated, nor can their relative importance be modified. As such, the model is representative of the conditions on Satory's tracks, that we assume to be fairly similar to those found on most freeways.

This model provides a frame loss probability depending of the distance and relative speed between two nodes (vehicles or RSUs); more precisely the model generates a *semi-linear frame loss profile*. A profile represents a single uninterrupted connection between two IVC devices and is used to determine the frame loss probability at any given distance, as long as they are within range (that is, as long as frame loss is under 100%). By using profiles, we focus on modelling individual instances of connection between two nodes, rather than simply modelling the average frame loss obtained over our total experimental measurements. A generic profile is shown in Fig. 4.

A profile is actually composed of two parts: a bell-shaped curve at first, followed by a linear regression; each part representing a different phenomenon. A profile  $\tau$  is described by equation 1:

$$\tau = \max \left[ A \cdot e^{B \cdot (d-C)^2} ; \min \left( \max [D \cdot d + E ; F] ; 1 \right) \right] \quad (1)$$

where  $d$  is the distance between the emitter and receptor.  $A, B, \dots, F$  are the model parameters estimated from empirical data.

The term  $A \cdot e^{B \cdot (d-C)^2}$  represents the frame loss area corresponding to the strongest ground reflection interferences,

centred at distance  $C$ . At this point the ground-reflected signal is strong enough to cancel out a large proportion of the incoming direct signal's energy, pushing a proportion of frames under the chipset reception's threshold; the frame loss corresponding to this proportion is represented by  $A$ . The bell curve's width is proportional to  $B$ ; note that  $B$  is always negative. The model assumes that no counter-measure is applied to reduce the frame loss induced by interferences at  $C$ .

The term  $D \cdot d + E$  is a linear regression where  $\tau$  is modelled linearly as a function of distance  $d$  and parameters  $D$  and  $E$ . This term represents the progressive increase of frame loss as received signal strength decrease. The increase starts from a non-zero frame loss ratio value given by parameter  $F$ , which represents the average of small perturbations measured within range. Typically,  $F$  will be low (less than 5%).  $D$  and  $E$  have two meaningful ratios: ratio  $\frac{F-E}{D}$  gives the distance at which frame loss starts to increase from the plateau at  $F$ ; ratio  $\frac{1-E}{D}$  expresses the distance at which frame loss reaches 100%, hence the maximum range.

We then created four classes, which are classified according to the relative speed between the emitter and receptor. The classes are:

$$\text{speed} = [0; 40], [40; 60], [60; 100], [100; 160]$$

The first speed interval is for equivalent speed between emitter and receptor. The last speed interval is dedicated to the opposite traffic direction, or for a scenario with one static actor and another dynamic one. The 2 last intervals represent other cases (acceleration, deceleration, overtaking, etc.).

For each class, the model's parameters  $A, B, \dots, F$  are estimated using the Levenberg-Marquardt algorithm for non-linear least squares [12]. Experimental data show that  $D$  and  $E$  are linearly correlated; the other parameters are assumed to be independent. The relationship between  $D$  and  $E$  is given by a Generalised Linear Model regression from the observed values of  $D$  and  $E$ :

$$E = \alpha D + \beta + e, \quad e \rightsquigarrow \mathcal{N}(0, \sigma) \quad (2)$$

For each parameter of the vector  $(A, B, C, D, F)^T$  applied to a specific class, a non-parametric probability density estimate is computed. The continuous distributions  $\mathbf{A}, \mathbf{B}, \mathbf{C}, \mathbf{D}, \mathbf{F}$  of each parameter of the vector  $(A, B, C, D, F)^T$  are computed with a Gaussian kernel smoothing method (the distribution  $\mathbf{E}$  of the parameter  $E$  can be obtained through its linear correlation with  $\mathbf{D}$ ).

The transponders' functions described in the previous subsection are kept with our new approach. However, when a receptor checks whether it is in range with transmitters, new tests are applied. At first, a frame loss profile is generated from parameters distributions selected from the appropriate class for the relative speed between the transmitter and the receptor. To reduce computational load, a new profile is generated only when the distance is under a certain threshold (typically, 1,000 metres).

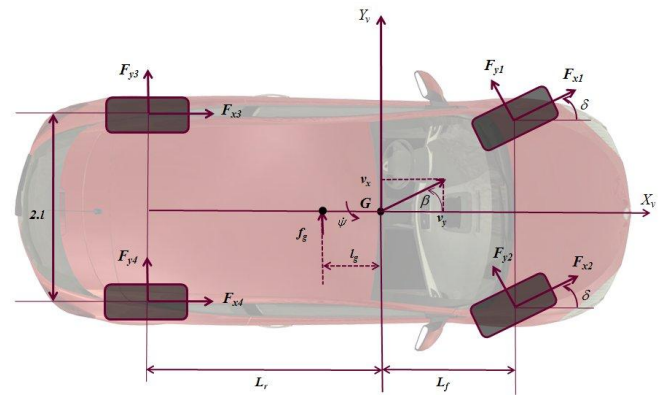


Fig. 5. Dynamic vehicle model

If a connection was previously established and lost for more than a certain duration (at least 30 seconds), a new profile is generated too.

After the profile is generated, the frame loss probability is extracted and the frame's success is tested against this value. In case of success, the receptor is allowed to read the frame's content according to the existing procedure. In the mean time, the profile is tagged as "active" and continues to be used for any frame exchange between these two specific transponders. If  $n$  is the number of transponders in the simulation, the maximum number of active profiles is thus  $\frac{n(n-1)}{2}$ .

Latency can be applied at this stage, by delaying the frame's extraction by a number of simulation steps. However, we have shown in [7] that point-to-point latencies remained overwhelmingly (99.47%) under 4 milliseconds for frames less than a 500 bytes (typical for EEBL applications). A simulation step is 5 milliseconds in SiVIC's default configuration, which means that short frame can be passed to the receptor transponder without delay. Nevertheless, if the simulation time is fixed to a lower value, then the latency mechanism could be activated.

We implemented a test mechanism based upon the amount of data which is encoded into the frame: if the amount is larger than a threshold (500 bytes), a delay is applied on the frame's data extraction. The number of simulation steps by which the frame is delayed is based on a simple linear regression from latencies measured experimentally. For example, a 500 bytes frame would be delayed by one step, which will provide a total latency of 10 milliseconds.

### E. Vehicles' control

SiVIC provides a parametric model developed by Sébastien Glaser [13] (see also [14]) for the dynamic behaviour of the vehicle chassis on the three axes (roll, pitch and yaw/heading). It also accounts for shock absorbers dynamics and non-linear tire road forces [15], [16]. Eventually, coupling between longitudinal and lateral axes, the impact of normal force variations, and the car alignment's moment are also integrated. The vehicle's chassis is modelled with an unbending suspended mass. This model allows installing, in a simple way, a large number of on-board sensors. We will use the notations of the chassis dynamics illustrated in Fig. 5.

In order to obtain the most accurate sensor data, comparatively to a real situation, it is necessary to both handle a vehicle dynamical model, and to simulate realistic actuator models. The actuators are motor and braking torques applied on each wheel, and the steering wheel angle. One can thus

deviation. If  $\delta(t)$  is greater than  $\delta_{max}$ , then we apply a saturation stage:

$$\delta(t) = \frac{\delta(t)}{|\delta(t)|} \times \delta_{max} \quad (5)$$

In our application, vehicles can be asked to follow the left, central or right lane during the simulation. If required, lane detection and tracking can be used instead of a track map, so that any simulated road can be used.

Longitudinal control has been improved from the previous architecture. Previously, vehicles were simply instructed to follow a certain speed, which was modified manually or from roadside beacons using the transponders simulation. This mechanism is kept, although it is now overridden by two additional controls.

Firstly, a mechanism is added in order to simulate an *interdistance regulation* process. As our typical demonstration scenario involves a platoon of several vehicles following each others, vehicles need to remain within acceptable interdistances at all times. On each vehicle, a pitch-stabilised narrow-beamed laserscanner is used to measure the distance to the leading vehicle. To maintain an acceptable interdistance, the vehicle's reference speed (or speed target)  $V_{ref}$  is computed with equation (6).

$$V_{ref} = V - [V \cdot (t_{inter} - t_h) - d_{target}] \times \frac{1}{t_{inter} - t_h} \quad (6)$$

where  $V$  is the vehicle's current speed,  $t_{inter}$  the minimum acceptable intervehicular time,  $t_h$  the driver's reaction time and  $d_{target}$  the distance to the closest obstacle, as measured by the laserscanner. This mechanism is used to simulate a simple human driver behaviour and the intervehicular time respected by the driver.

For the leader vehicle, the reference speed is extracted from frames received from the infrastructure transponders. When a receiver attached to the leader vehicle receives the new speed information, the following control is applied:

$$Ct = 3 \times R \times M \times (V - V_{ref}) \quad (7)$$

where  $Ct$  is the torque order applied to the front wheels,  $R$  the wheel's radius, and  $M$  the chassis' mass.  $V$  is the leader vehicle's speed and  $V_{ref}$  is the reference speed. For a follower vehicle, the same equation is used but with  $V_{ref}$  computed from equation (6).

A second approach has been developed in order to maintain a Time To Collision (TTC) around 2 seconds. From a speed  $V_f$  (follower vehicle's speed), the distance required to maintain the 2 seconds TTC is  $D(t) = V_f(t) \times 2.0$ . Then, the safety distance is  $e = D_{lf}(t) - D(t)$ , where  $D_{lf}$  is the vehicular interdistance between a leading vehicle and its follower. The "safety speed"  $\dot{e}$  is also estimated. From there, the control applied to the wheels is computed as follows:

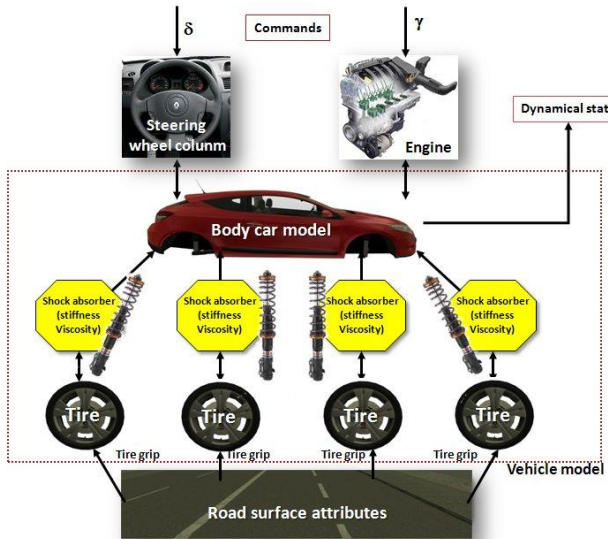


Fig. 6. Vehicle model in the SiVIC platform with its attributes

simulate front wheel drive, rear wheel drive or four wheels drive.

Figure 6 shows the model's level of complexity, and the links between all the different physical modules involved in it. Each module is completed with a list of available parameters. These parameters can be modified during the simulation. Vehicles' control is based on the same architecture as described in [5]. Vehicles are controlled longitudinally by torques on the wheels and laterally by the steering wheel angle; controls are decoupled.

Similarly to the previous architecture, lateral control is performed with an accurate map of the test track: angular and lateral deviations from the vehicle's lane are computed from this map. The controller uses the road's curvature at the vehicle's position, the inter-axes distance, and the angular and lateral deviations as described by equation (3):

$$\delta(t) = \tan^{-1}(L \times K(t)) \quad (3)$$

with

$$K(t) = K_{ref}(t) - [\mu_{\perp} \times (\psi - \psi_{ref}) + \lambda_{\perp} \times e_{\perp}] \quad (4)$$

In the previous lateral equations (3) and (4),  $\delta(t)$  is the lateral steering angle,  $L$  is the inter-axle distance, set at 2.58 metres.  $K(t)$  is the correction term on the vehicle's curvature, depending on the road's curvature. This correction depends of two suitable gains  $\mu_{\perp}$  and  $\lambda_{\perp}$ .  $\psi$  and  $\psi_{ref}$  are, respectively, the vehicle's yaw angle and the road's heading.  $e_{\perp}$  is the lateral

$$Ct = M \times R \times (Kp \times e + Kd \times \dot{e}) + \sum_{i=1}^4 I_i \times \dot{\omega}_i \quad (8)$$

With  $\dot{\omega}_i$  the derivative speed of wheel  $i$ ,  $Kd$  the derivative gain and  $Kp$  the proportional gain. Suitable values have been set for  $Kd$  and  $Kp$ . If  $Ct$  is negative, then the current manoeuvre is a deceleration, and  $Ct$  is applied to the four wheels ( $Ct/4$ ). If  $Ct$  is positive, then the current manoeuvre is an acceleration, and the torque order is applied only to the front wheels ( $Ct/2$ ).

Secondly, we have an *emergency regulation* mechanism. This mechanism is triggered only on IVC-equipped vehicle, when an emergency braking frame is successfully received and decoded by the receptor. Immediate or delayed reaction can be chosen, allowing simulating either a reactive or informative system (i.e. one with automated braking versus one that simply flashes an alert to the driver). In the former,  $V_{ref}$  is simply set to zero immediately after the frame is decoded. In the latter case,  $V_{ref}$  is only updated after a  $t_h$  delay has passed. At the moment, the only way for the vehicle to not brake is to miss the emergency braking frame. A future extension will allow a more realistic behavior with a context-aware, so that vehicles which are far away from the actual event (e.g. more than 500 metres) and still receive an emergency braking frame either ignore it, or enter into a state of heightened alert (where  $t_h$  is decreased and  $t_{inter}$  increased). The leader vehicle has a similar mechanism for the initial emergency braking, which is triggered when its curvilinear abscissa on the tracks reaches a user-defined value.

### III. COOPERATIVE COLLISION WARNING PROTOTYPING

We implemented an EEBL/CCW application with our architecture, which was inspired from the scenario studied in [17], [9], [10]. Results from [9] showed that only a small percentage of IVC-equipped vehicles was necessary in a vehicles platoon to considerably reduce the number of crashes, which was confirmed in [10]. For example, in dense configuration, only 5% of equipped vehicles were sufficient to reduce the number of crashes by two thirds in an emergency braking scenario compared to completely unequipped scenario. We will show how our architecture can reproduce these previous results (on a smaller scale) and show that they can be refined when a more detailed simulation architecture is available.

The previous studies used heavily constrained strings or platoons of vehicles. However, the interest of this architecture is its capacity to generate generic and non repeatable configurations in order to be closer from reality. Thus, we will use a scenario which is less constrained and non-repeatable. That way, we will be able to compare our results and previous studies, and test whether the results from previous studies still hold when the vehicles platoon behaved more realistically. As we will see later on, this is not completely the case.

We set up a scenario which is identical in practice to the scenario studied in [9], [10], with the only difference being the reduced size of the vehicles' platoon. The granularity of our results will be limited compared to studies using larger strings, but it should not be an impairment to the validation of our CS simulation architecture.

A five vehicles platoon (1 leader, 4 followers) is set up in SiVIC, in the virtual reproduction of Versailles-Satory's test track called *la routière*, modelling a French non segregated trunk road (*route nationale*). Each vehicle can be configured individually and independently, but for the sake of simplicity, we will keep an homogeneous fleet in terms of acceleration, braking capacity and reaction time ( $t_h = 0.5$  second). The same was true in [9], [10]. Additionally, the vehicles are set in reactive mode: there is no delay between the reception of an emergency frame and the beginning of the braking action. All vehicles have  $t_{inter} = 2.5$  seconds; except  $veh_2$  for which  $t_{inter} = 1.5$  seconds, in order to simulate a slightly more risked driving. According to government statistics, more than half (56.4%) of the drivers do not follow safe interdistances recommendations (at least 2 seconds) in dense traffic [18]. All these parameters are either controlled from RTMaps platform (where they can be changed online), or in the SiVIC script, which is loaded once at start-up.

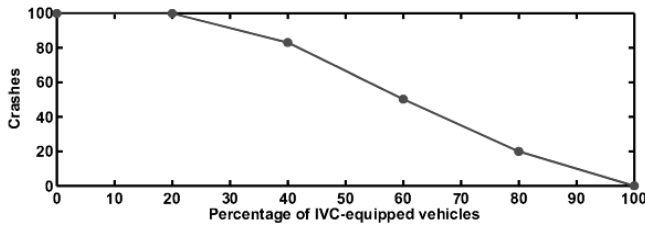
The vehicles start with a static configuration and all grouped together in one location of the track. From these starting positions, the vehicles arrange themselves in a platoon on the right-hand lane, and progressively speed up to 70 km/h. While the starting positions are always identical, the interdistance regulation at very short distances means that at each instances there are varying interdistances between the five vehicles; each scenario's instance forms a different platoon. Follower vehicles are equipped with telecommunication receptors, depending on the desired equipment ratio. IVC equipment is randomly selected for each individual follower. The equipment is reset at each new run. The emergency braking event takes place in a long straight section approximately 700 metres after the starting position.

The scenario was replayed at least one hundred times for each of the following equipment ratios: 0/5, 2/5 (leader + 1 follower), 3/5, 4/5, and 5/5. The  $\rho = 1/5$  case is not simulated as it corresponds to having only the leader vehicle equipped, which is not different from  $\rho = 0/5$  in this scenario. A total of 716 runs were simulated, which generated 1197 crashes. The following variables were recorded for all vehicles: curvilinear abscissa, TTC (Time To Collision), the distance from the obstacle  $d_{target}$ , the ego-vehicle speed  $V$ , the speed reference  $V_{ref}$ , emergency frame broadcast and instances of collisions.

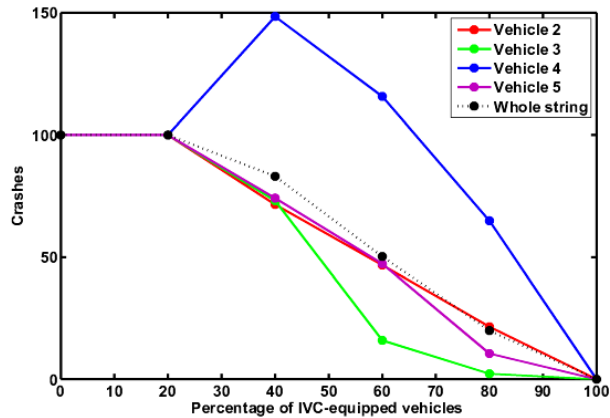
#### 1) Crashes number analysis

Fig. 7a shows the normalised total rear-end crashes at different equipment ratios. By introducing 2 IVC-equipped vehicles ( $\rho = 2/5$ , or 40%), the number of crashes fell by 17%; with  $\rho = 3/5$ , the crashes fell by 50%, and with  $\rho = 4/5$ , the crashes fell by 80%. In a completely equipped platoon, no crashes were recorded. Note that the crashes number is maintained at 100% for  $\rho = 1/5$  since it is indistinguishable from  $\rho = 0/5$ .

As we already stated, in [9], [10] the number of vehicles in the string was significantly higher, which allowed for a better granularity of  $\rho$ . Compared to the repeatable scenario however, the large number of simulation runs make it possible to obtain more refined, and more realistic, results. Contrary to [10], our results do not show a strong  $1/x$  type decrease of



(a) Normalised crashes count for the whole string



(b) Normalised crashes count for the whole string and each individual vehicle

Fig. 7. Illustrations of the reduction in crashes obtained by introducing IVC in the vehicles string

crashes when the IVC equipment ratio increases. However, they follow the same trend; for example, at a 2,600 vehicles/hour capacity, the reduction in crashes' number from  $\rho = 0\%$  to  $\rho = 80\%$  is very similar to our results. Furthermore, it can be noted that in our scenario, IVC equipment starts to provide a reasonable safety increase with only more than 50% of equipped vehicles. This difference can

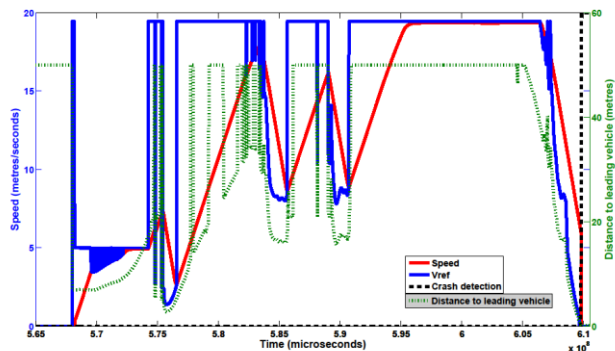


Fig. 8. Detailed variables measurements for one vehicle during a simulation run

be attributed to the different methodologies applied to the studies. Nonetheless, our results are coherent with the EEBL scenario and shows that our CS simulation architecture can be used to complement larger simulations like [10], notably by providing more detailed analysis. Indeed, being able to record

and study variability inside the platoon, for each individual vehicle, is a major improvement brought by the architecture. Different kinds of data can be considered for study, which will be shown with two examples. Typically, it is possible to extract information on the behaviours of each vehicle. This can concern the behaviour of a vehicle during a single run (our first example), or crash patterns associated with them over the whole experimental runs (our second example).

On one hand, we can focus on a single vehicle behaviour. For example, Fig. 8 shows the interdistance regulation variables for *veh<sub>3</sub>*, taken during a  $\rho = 3/5$  run. In this run the *veh<sub>3</sub>* was not equipped with an IVC device.  $V_{ref}$  is shown by the blue curve (left-hand axis). It depends either on limit speed instructions from RST (Road Side Transponder) or on  $d_{target}$ , shown by the green dotted curve (right-hand axis), via equation (6). The quick distance variations visible on this figure usually happen when the preceding vehicle is turning, and so leaves the narrow field of view of the frontal laserscanner. One can also note, just after the  $5.7 \times 10^8$  timestamp, a brief period for which  $V_{ref}$  fluctuates a lot, very quickly. This is a visual representation of the interdistance regulation behaviour that leads to the scenario's non-repeatability.

$V$  (red curve, left-hand axis) is well regulated according to  $V_{ref}$ . At the end of the run, we can note that the vehicle starts to brake because  $d_{target}$  becomes too small; the delay introduced by the human reaction time is clearly visible: when the vehicle starts to brake, the interdistance has already shrunk by more than 10 metres. Even at maximum braking power, *veh<sub>3</sub>* cannot stop before the impact with the preceding vehicle, which is shown by the vertical black dotted line. The impact takes place at the relatively slow speed of 6 metres.seconds<sup>-1</sup> (~22km/h).

On the other hand, we can focus on whole runs. Fig. 7b reproduces Fig. 7a data (the dashed black curve), and overlays it with the normalised crashes counts for each individual vehicle. From this figure, it is easy to see that when the IVC equipment grows then the number of crashes decreases. However, it seems not to be necessarily the case for individual vehicles. Indeed, for *veh<sub>4</sub>* and the scenario having 40% of IVC equipment, we observe a 47% increase in the number of crashes encountered by this vehicle. At 60% equipment ( $\rho = 3/5$ ), the crash count is still 15% higher than in a fully non-equipped scenario. At 80% equipment, *veh<sub>4</sub>* benefited from IVC the same way that other vehicles benefited for 40% equipment.

Taken at face value, this result would suggest that while drivers would collectively benefit from using EEBL, some drivers unfortunately would see their crash likelihood increase. Obviously, this is an unacceptable conclusion in terms of road safety. It is further aggravated knowing that, if the absolute number of crashes is considered, *veh<sub>4</sub>* is the one with the least crashes at  $\rho = 0/5$ . How could introducing IVC make the previously safest vehicle the least safe? Further investigations show this is unlikely to happen in an actual on-road situation.

Indeed, from the detailed recordings, *veh<sub>4</sub>* appears to be following *veh<sub>3</sub>* with an interdistance slightly above average. In the scenario without IVC, this is not an issue and the vehicle manages to stop before colliding with *veh<sub>3</sub>* in most cases,

hence its lower number of crashes relatively to the others. On the other hand, at  $\rho = 2/5$ , if  $veh_2$  or  $veh_3$  are equipped with IVC,  $veh_3$  will have a tendency to brake earlier than it did in the non-equipped scenario. Because of this, the relative speed between the two vehicles is large when  $veh_4$ 's controller starts to brake. In that case, even at maximum braking capability,  $veh_4$  is unlikely to be able to stop before colliding with  $veh_3$ , which leads to the 50% increase in crashes we measured.

Unfortunately, this behaviour stands out as a limitation of our simulation. Indeed, on a real road,  $veh_4$ 's driver would become aware of  $veh_3$ 's braking manoeuvre with the activation of its braking lights;  $veh_4$  would thus brake much earlier than what the current controller decides to do. At the moment, our architecture cannot simulate this behaviour. Our scenario is thus artificially increasing crashes for that specific vehicle.

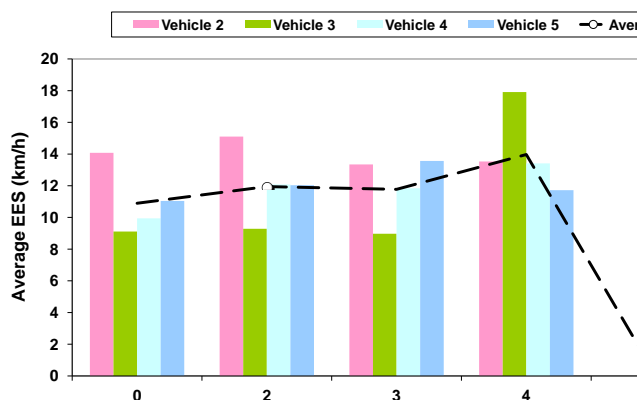


Fig. 9. Average EES computed for each and all vehicles, at different values of  $\rho$

Nonetheless, this happens only with  $veh_4$ , which do not invalidate the results for the whole platoon. All the remaining vehicles behaved according to the scenario's expectations. Additionally, if we filter the runs to keep only the ones where  $veh_4$ 's interdistance is comparable to the string's average,  $veh_4$  behaves like the other vehicles. Also note that  $veh_2$ 's count is higher than the others on average (ignoring  $veh_4$ ) because of its more aggressive driving style, which is consistent with the scenario's setting.

## 2) Crashes severity analysis

Thanks to SiVIC's realistic vehicle motion models, we can estimate the severity of crashes from the EES (Equivalent Energy Speed), which is the energy dissipated by the velocity change when a vehicle is hitting an obstacle. This analysis is made in post-processing based on the vehicle's variables recorded during the simulation runs.

Interestingly, the EES results (Fig. 9) show that while increasing IVC equipment leads to less crashes, it does not reduce the remaining crashes' severity, except for complete equipment where no crash took place. The dispersion of individual averages does not allow concluding that severity actually increased. However, the severity is demonstrably not decreasing, contrary to what was found in previous studies (unless of course when  $\rho = 5/5$  where there is no crash). A look into the detailed distribution of EES for each individual vehicle confirms this lack of improvement. The shapes of the

EES distribution fluctuate, but the averages remain relatively stable or can even increase in some case

Note that the  $veh_3$  outlier (94% increase) at  $\rho = 4/5$  is computed from only two crashes on 224 runs. In the two runs where it crashed,  $veh_3$  was following the preceding vehicle very closely to the minimum acceptable interdistance, and thus did not have the time to react properly during the emergency braking event. If the standard deviation is small for this vehicle, it is because the two crashes took place in runs that happened, by chance, to be almost exact repetitions.

While the EES absolute values remained largely under any dangerous threshold due to the scenario's conditions, implications are worrying at higher speeds. Indeed, from the point of view of a system's contribution to road safety, it is better to have several weak crashes, where no driver is injured, then one or two violent ones, where there are fatalities. In [9], it was shown that using the raw crashes number to evaluate IVC's contribution to the platoon's safety was always more pessimistic than using an EES-based severity criterion. However, we found here that while the number of crashes indeed significantly decreased, the remaining crashes' severity did not decrease. In this case, a crashes number-based criterion would have been considerably more optimistic than the EES-based severity criterion.

## IV. CONCLUSIONS AND FUTURE WORKS

In this paper we have presented a cooperative systems simulation architecture, developed within the SiVIC-RTMaps™ interconnected platforms. This architecture uses the SiVIC-RTMaps™ capabilities to provide very realistic simulations, and has several improvements on previous architectures developed at LIVIC. The two main improvements concern: (1) firstly, the introduction of an empirical modeling of 802.11p IVC system based on ground-truth data collected on the Satory's test tracks; and (2) secondly, an improved vehicle controller, allowing for an automated vehicle to behave more like a human-driven one. The many variables accessible in great details, supported by realistic physical models (e.g. for vehicle's motion), also provide an improvement on pre-existing simulations, so that the behaviour of individual vehicles can be studied.

We validated this architecture by reproducing results from previous researches on the contribution of IVC to the reduction of rear-end crashes in vehicle platoons, with a caveat. Compared to these previous results, our architecture allows diving into greater details into each vehicle's behaviour, as many different variables are accurately recorded. Individual statistics can be generated for each vehicle. We have used these functionalities to evaluate the severity of each individual crash (a total of 1197, over 716 runs of a 5-vehicles string), via the computation of the Equivalent Energy Speed (EES). This more detailed study has yielded unexpected results: while introducing IVC decreases the number of crashes as expected, the average EES does not decrease. This means that the remaining crashes' severity remain constant. These results need to be further confirmed, in which case they would raise a few concerns about the actual safety benefits of IVC. It is often assumed that IVC will also help to reduce the severity of crashes, and that in some cases it might be more beneficial to

favour this effect rather than simply reducing crashes numbers. If some benefits can be expected from the reduction of crashes that we obtained, our results show that the efficiency of an EEBL application to reduce crashes severity might have been over-estimated. Effectively, the safety benefits of IVC for road users are not as important as initially expected. Earlier results suggested that introducing IVC would lead to less crashes, and that the remaining crashes would be less severe. Our results suggest that, indeed, there will be fewer crashes. However, the remaining crashes will remain as severe as previously.

Further work should concern determining whether the absence of improvement of severity is a by-product of our scenario's setting, and continuing on improving the architecture's functionalities. A new control mechanism is required to better reproduce drivers' behaviour when the emergency event is taking place more than a few dozen metres in front of them. Related to this issue, vehicles currently react immediately to the reception of an emergency braking frame, both in reactive or informative modes, which just modulate the reaction's delay. Thus, equipped vehicles located several hundred metres away from the initial perturbation will also start to brake, when that is, in most cases, not necessary. In further studies, we will limit the immediate reaction to a certain radius around the initial perturbation. Vehicles outside this radius will be put into a state of heightened alert, by increasing  $t_{inter}$  and decreasing  $t_h$ . Moreover, we will test the impact of degraded vehicle dynamic conditions like low tires adherence, low braking capacities, strong acceleration capacities, etc. in such an IVC safety systems.

#### ACKNOWLEDGEMENT

This work is supported by the Commonwealth of Australia through the Cooperative Research Centre for Advanced Automotive Technology, as well as by the French Institute of Science and Technology for Transport, Development and Networks. A sub part of this work has been developed in the CooPerCom project, a 3-year international research project (Canada-France). The authors would like to thank the National Science and Engineering Research Council (NSERC) of Canada and the Agence nationale de la recherche (ANR) in France for supporting the project.

#### REFERENCES

- [1] S. Demmel, D. Gruyer, and A. Rakotonirainy, "V2V/V2I augmented maps : state-of-the-art and contribution to real-time crash risk assessment," in 20th Canadian Multidisciplinary Road Safety Conference. Hilton Niagara Falls, Ontario: The Canadian Association of Road Safety Professionals, June 2010.
- [2] A. A. Carter, "The status of vehicle-to-vehicle communication as a means of improving crash prevention performance," National Highway Traffic Safety Administration, Tech. Rep, pp. 01–19, 2005.
- [3] D. Gruyer, S. Glaser, and B. Monnier, "SiVIC, a virtual platform for ADAS and PADAS prototyping, test and evaluation," in FISITA World Automotive Congress, June 2010.
- [4] D. Gruyer, S. Glaser, S. Pechberti, R. Gallen, and N. Hautiere, "Distributed simulation architecture for the design of cooperative ADAS," in First International Symposium on Future Active Safety Technology toward zero-traffic-accident, September 2011.
- [5] D. Gruyer, S. Glaser, B. Vanholme, and B. Monnier, "Simulation of automatic vehicle speed control by transponder-equipped infrastructure," in 9th International Conference on Intelligent Transport Systems Telecommunications, October 2009, pp. 628–633.
- [6] IEEE Computer Society, "IEEE standard for information technology - telecommunications and information exchange between systems - local and metropolitan area networks - specific requirements part 11: Wireless LAN medium access control (MAC) and physical layer (PHY) specifications - amendment 6: Wireless access in vehicular environments," New York, 2010.
- [7] S. Demmel, A. Lambert, D. Gruyer, A. Rakotonirainy, and E. Monacelli, "Empirical IEEE 802.11p performances evaluation on test tracks," in IEEE Intelligent Vehicles Symposium, 2012.
- [8] D. Gruyer, S. Pechberti, and S. Glaser, "Development of full speed range acc with sivic, a virtual plateforme for adas prototyping, test and evaluation ADAS," in IEEE Intelligent Vehicles workshop, june 2013.
- [9] B. Mourllion, D. Gruyer, and A. Lambert, "A study on the safetycapacity tradeoff improvement by warning communications," in IEEE Intelligent Transportation Systems Conference, September 2006, pp. 993–999.
- [10] A. Lambert, D. Gruyer, A. Busson, and H. M. Ali, "Usefulness of collision warning inter-vehicular system," International Journal of Vehicle Safety, vol. 5, no. 1, pp. 60–74, 2010.
- [11] B. Steux, "RTMaps, un environnement logiciel dédié à la conception d'applications embarquées temps-réel. utilisation pour la détection automatique de véhicules par fusion radar/vision," Ph.D. dissertation, Écoles des Mines de Paris, 2001.
- [12] J. Moré, "The Levenberg-Marquardt algorithm: Implementation and theory," in Numerical Analysis, ser. Lecture Notes in Mathematics, G. Watson, Ed. Springer Berlin / Heidelberg, 1978, vol. 630, pp. 105–116.
- [13] S. Glaser, "Modélisation et analyse d'un véhicule en trajectoires limites. application au développement d'un système d'aide à la conduite," Ph.D. dissertation, Université d'Evry Val d'Essonne, 2004.
- [14] N. Kiencke and L. Nielsen, Automotive Control Systems: For Engine, Driveline and Vehicle. Springer Verlag, 2004.
- [15] H. Dugoff, P. Fancher, and L. Segel, "An analysis of tire traction properties and their influence on vehicle dynamic performance," SAE Technical Paper, Tech. Rep., 1970.
- [16] R. Rajamani, Vehicle Dynamics and Control. Springer USA, 2006.
- [17] M. Mangeas, "Rapport d'activités, livric," IFSTTAR (LIVIC), Tech. Rep., 2003.
- [18] Observatoire national interministériel de la sécurité routière, "La sécurité routière en france - bilan de l'année 2010," Paris, 2011.